Ductile Concrete Material with Self-Healing Capacity for Jointless Concrete Pavement Use

Zhigang Zhang, Shunzhi Qian, Hezhi Liu, and Victor C. Li

The existence of joints in concrete pavement tends to cause many distresses and driving discomfort, thus resulting in high maintenance and shortened service life. This study achieved jointless function in concrete pavement by utilizing the high ductility and self-healing capacity of engineered cementitious composite (ECC). From the preliminary experimental results, ECC showed high strain capacity of 4.4% and deflection capacity of 7.9 mm under tension and bending, overcoming the brittleness of normal concrete. The flexural and compressive strengths of ECC are 12.2 and 45.8 MPa, respectively, which could meet the requirements of heavy-duty concrete pavement in accordance with design guidance in China. Under restrained shrinkage, ECC also shows a very low tendency to form fracture failure. In addition, the self-healing phenomenon is observed in ECC. Its stiffness, tensile strain capacity, tensile strength, and resonant frequency value show a very high recovery level after self-healing, nearly approaching that of virgin ECC of the same age. The water permeability coefficient of predamaged ECC decreases gradually with self-healing age, and eventually is close to that of the undamaged specimens. Based on the experimental results, it is concluded that ECC material, as expected, has the potential to be used in jointless concrete pavement.

As one of the main pavement types, concrete pavement has undergone rapid development in the past 20 years in China, taking up about 70% of the entire paved roads and 10% of highways, due to the high load-bearing capacity, long service time, and relatively low cost of concrete pavement. However, there are also many defects in concrete pavement, which greatly limit its expansion on expressways. The joints are essential for the concrete pavement to prevent cracking from drying shrinkage and temperature variations. As the weak spots in pavement, the joints can cause many distresses (slab faulting, pumping, edge failure, and so forth) and driving discomfort. For instance, cracking, which is inherent in concrete pavement because of its brittleness, allows water to penetrate and subsequently erode the pavement base due to dynamic water pressure, eventually resulting in fracture of unsupported pavement panels. During the service life, the joints require extensive maintenance work, which gives rise to significant traffic delays. The maintenance work also tends to be very expensive and time consuming, because of the high strength and long-time curing of newly cast concrete pavement.

To enhance the service life and durability of concrete pavement, jointless concrete pavement was proposed to avoid distresses and driving discomfort. Normally, continuously reinforced concrete pavement (CRCP) and prestressed concrete pavement (PCP) have been used to achieve jointless and crack-controlled concrete pavement. Nonetheless, although overall integrity is enhanced, the pavement structure of CRCP is still largely permeable to water, because of CRCP's inability to control crack width, thus shortening its service life. PCP could arrest the appearance of cracks, but the construction process is complicated and the construction quality is difficult to control. In addition to these drawbacks in CRCP and PCP, the rebar and prestressed tendon would still have the problem of deterioration coming from the penetrated aggressive agents. When the steel rebar inside the concrete corrodes, it will expand and place more pressure on the surrounding concrete, leading to further cracking and spalling. This paper proposes a ductile concrete material, engineered cementitious composite (ECC), as a candidate material for jointless concrete pavement.

ECC is a kind of high-performance, fiber-reinforced cementitious composite (HPFRCC), designed by Li in the 1990s based on micromechanics theory (*1*). ECC develops multiple microcracks along the specimens under tension, meanwhile retaining the crack width within 60 μm. This contributes to the high tensile strain capacity of ECC, ranging from 3% to 5%, which is 300 to 500 times that of normal concrete (*2–5*). The high ductility and crack width control capacity of ECC can accommodate the deformation caused by drying shrinkage and temperature change without causing localized fracture. The tight microcrack in ECC is expected to have little impact on water transport property and structural durability, given that the water permeability coefficient and chloride diffusion property of concrete with crack width less than 200 μm were found to be nearly the same as those of uncracked concrete (*6–8*). Therefore, this kind of tight microcrack in ECC is expected to have little impact on the water transport property and durability compared with the millimeter-size cracks typically found in normal concrete. More interestingly, under certain circumstances (e.g., when rainwater and carbon dioxide are available), a microcrack in ECC can heal itself because of the further hydration of unhydrated cement and secondary reaction of fly ash (*5, 9*).

The self-healing properties of pavement materials could potentially counteract the continuous deterioration of cracks, thus reducing repair times and total construction cost. Furthermore, these properties are also beneficial in decreasing the greenhouse gas emissions and energy

Z. Zhang, Key Laboratory of New Technology for Construction of Cities in Mountain Area (Chongqing University), Ministry of Education, 400045 Chongqing, China. S. Qian, School of Civil and Environmental Engineering, Nanyang Technological University, Singapore, 639798; H. Liu, College of Water Conservancy and Hydropower Engineering, Hohai University, Nanjing 210098, China. V. C. Li, Department of Civil and Environmental Engineering, University of Michigan, 2350 Hayward Street, Ann Arbor, MI 48109-2125. Corresponding author: V. C. Li, vcli@umich.edu.

Transportation Research Record: Journal of the Transportation Research Board, No. 2640, 2017, pp. 78–83.
http://dx.doi.org/10.3141/2640-09

consumption caused by traffic congestion due to pavement repair (*10*). The self-healing behavior of ECC pavement not only closes the path for water ingress (*5, 11*), protecting the pavement base from damage caused by water scour, but also recovers its tensile or flexural mechanical properties (*9*). As a result, ECC is expected to extend the service life of pavement structures significantly.

Based on this discussion, the high ductility, crack-width control capacity, and self-healing property of ECC make it a feasible candidate material to be used in jointless pavement material. This paper describes the mechanical (compression, tension, and bending) properties of ECC designed for pavement application. The paper then summarizes the cracking resistance of ECC under restrained shrinkage, and reports the influence of self-healing behavior on the tensile properties and water permeability of ECC material.

EXPERIMENTAL PROGRAMS

Materials and Mix Proportions

In this study, the ingredients for ECC material included Type I portland cement, fly ash, silica sand, water, polyvinyl alcohol fiber (39 µm in diameter, 12 mm in length), and polycarboxylate-based high-range water reducer. To ensure the even dispersion of fibers in ECC paste and control the cracking pattern, fine silica sand with average particle size of 110 µm was used in ECC instead of the coarse aggregate usually found in normal concrete. The elimination of coarse aggregate results in much higher binder content in ECC compared with normal concrete. As an industrial byproduct, a large volume of fly ash can be incorporated into ECC for partial replacement of cement, resulting in enhanced material greenness and reduced cost.

The mix proportion of an ECC without air entrainment designed for pavement use is listed in Table 1. The ECC mixture has a water–binder ratio of 0.25, fly ash–cement ratio of 2.2, and silica sand–cementitious materials (cement and fly ash) ratio of 0.36.

The mixing process followed typical ECC mixing procedures, which were found in the literature (*12, 13*). After casting, the specimens were cured under plastic sheet cover for 24 h before demolding. Then the specimens underwent continued curing in lab air at room temperature of 20±3°C and relative humidity 40% ±5% for 27 days before testing.

Specimen Preparation and Testing

Measurement of Mechanical Properties

The mechanical properties (compressive, tensile, and bending behavior) of ECC were evaluated by the compressive, uniaxial tensile, and four-point bending tests, respectively. The compressive strength of ECC was obtained by averaging the results of three cubic specimens with dimensions 50.8 × 50.8 × 50.8 mm, in accordance with ASTM C109 (*14*).

TABLE 1 Mixture Proportion of Pavement with ECC Mixture

Cement	393
Fly ash	865
Silica sand	457
Water	311
High-range water reducer (HRWR)	5
Polyvinyl alcohol (PVA) fiber	26

NOTE: Values are in kg/m^3.

The uniaxial tensile test and four-point bending test were conducted under quasi-static condition with deformation control of 0.5 mm/min at loading point. The detailed test procedure and dimensions of dog bone–shaped specimens for tensile tests followed the Japan Society of Civil Engineers recommendations for design and construction of HPFRCC with multiple fine cracks (*15*). For the four-point bending test, the full span length was 300 mm, with a middle span of 100 mm. The dimensions of the beam specimen for the bending test were 305 mm (length) × 76 mm (width) × 38 mm (height).

Evaluation of Self-Healing Behavior

The recovery of tensile properties and change of water permeability after the self-healing process were investigated to reveal ECC's self-healing behavior. The uniaxial tensile test was adopted to reveal the effect of self-healing on the recovery of ECC's tensile properties. The ECC specimens were preloaded to two damage levels with tensile strain of 1% and 2%. The predamaged specimens were immersed in water for 1 day and then exposed in air for 1 day, which is defined as one wet–dry cycle. This cycle simulates the exposure of pavement to the natural environment, which typically involves rainfall and drying. The recovery levels of the tensile properties of the damaged specimens contributed by self-healing were compared with those from virgin specimens (control case).

After every wet–dry cycle, the resonant frequency (RF) of the specimens was measured based on ASTM C215 (*16*). Normally, the RF measurement is a method to monitor the damage level of concrete after experiencing freezing-thawing. In this study, it was used to observe the recovery level of predamaged ECC specimens with a self-healing process. The normalized RF provides the change of RF in preloaded ECC specimens during the self-healing process, which is calculated according to the following equation:

$$RF_{\text{normalized}} = \frac{RF_{\text{preloaded}}}{RF_{\text{virgin}}} \times 100\% \qquad (1)$$

where

$RF_{\text{preloaded}}$ = RF value of preloaded specimens that underwent the self-healing process and
RF_{virgin} = RF value of control specimen without preloading.

To remove the effect of further hydration or moisture content changes during wet–dry cycles on RF recovery, the undamaged specimens also underwent wet–dry cycles, to have the same exposure condition as that of the preloaded specimens. A normalized RF value of 100% implies a full recovery of the preloaded ECC specimen from crack damage.

The influence of ECC's self-healing behavior on water permeability was evaluated by the falling head water permeability test. The coefficient of permeability of specimens was calculated based on Darcy's law. Figure 1 shows the detailed experimental setup for this test. In previous studies, the specimen in this test was unloaded, which can potentially cause 80% recovery of crack width when compared with that of a loading specimen (*8*). The change in crack width has a great impact on the concrete's transport properties, as the water flow rate is proportional to the cube of the crack width (*17*).

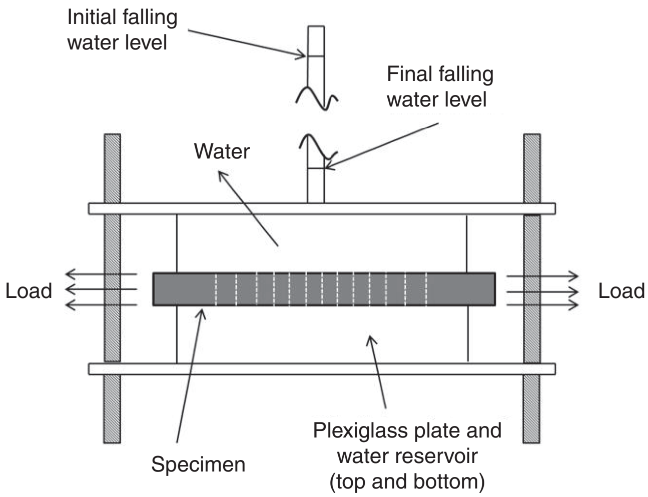

FIGURE 1 Experimental set-up for the water permeability test.

To simulate the practical crack open status for ECC pavement in service, the specimen loading was retained during the permeability test with a special device developed by Liu et al. (*18*). Before the permeability test, the ECC specimen was first preloaded to 1% tensile strain to produce cracks. All the crack widths were recorded by optical microscope. After preloading to 1% tensile strain, 14 microcracks were observed along the ECC specimen, with average crack width of 43 µm.

RESULTS AND DISCUSSION

Mechanical Performance of Pavement with ECC

During pavement structural design, the mechanical properties of pavement materials are specified as very important parameters. According to the concrete pavement design standards in China (*19, 20*), for roads with heavy traffic, the compressive strength and flexural strength of the pavement material are required not to be less than 40 and 5 MPa, respectively.

Figures 2 and 3 present the tensile and flexural performance of ECC material, respectively. As shown in the figures, unlike the brittle failure of normal concrete, ECC exhibits highly ductile behavior under tension or bending. All the curves can be divided into two stages before sudden load drop corresponding to fracture failure. First, the ECC specimens undergo a linear elastic stage under tension or bending before formation of the first crack. Afterward, the ECC enters a metal-like strain or deflection hardening stage by developing multiple cracks. The maximum tensile or flexural stress on the curves is defined as the tensile or bending strength of the ECC material. The corresponding strain or load point displacement at peak stress is defined as the tensile strain or deflection capacity of the ECC.

The table below summarizes the mechanical properties of ECC under tensile, bending, or compression loading. As shown in this table, due to the fiber-bridging effect between two crack faces, the tensile strength of ECC is 5.8 MPa, which is about two times that of normal concrete with C45 grade compressive strength. The tensile strain capacity of ECC reaches 4.4%, which is more than 400 times that of conventional concrete. This high ductility is adequate to accommodate the deformation caused by drying shrinkage and temperature change, allowing for jointless design on highways. Figure 4 illustrates the crack pattern of ECC under tension, where many microcracks appear along the specimen length with crack width less than 80 µm.

Mechanical Property	*ECC Value*
Tensile strength	5.8 ± 0.5 MPa
Tensile strain capacity	4.4% ± 0.3%
Flexural strength	12.2 ± 0.7 MPa
Deflection capacity	7.9 ± 0.2 mm
Compressive strength	45.8 ± 2.5 MPa

The flexural strength and compressive strength of ECC are 12.2 and 45.8 MPa, respectively, satisfying the requirements of concrete pavement material. Because of the higher flexural strength and lower

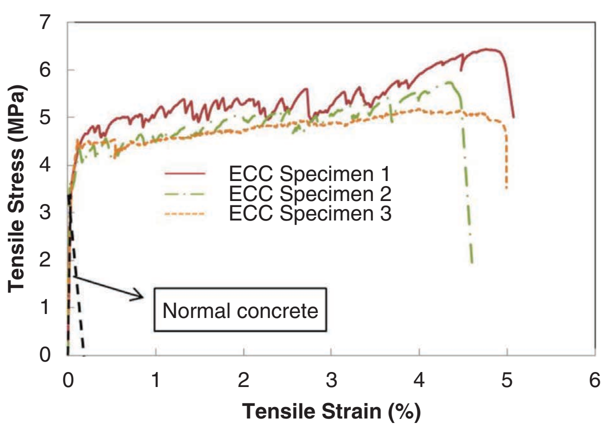

FIGURE 2 Tensile stress–strain relationship of ECC under tension.

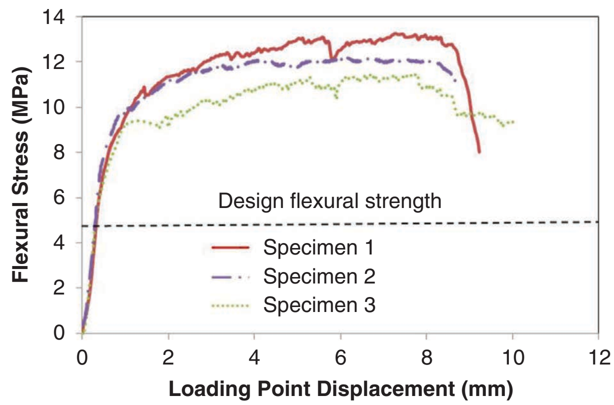

FIGURE 3 Flexural stress-deflection relationship of ECC.

FIGURE 4 Crack pattern of ECC under tension.

stiffness of ECC material, the thickness of ECC pavement could be one-third that of normal concrete to achieve equal or greater fatigue life (*21*). The deflection capacity of ECC under bending reaches 7.9 mm, which is much greater than that of normal concrete with no inelastic deformation capacity. This large bending deflection capacity allows ECC pavement to adjust its vertical deformation caused by temperature gradient along depth direction, which will help avoid fracture failure of pavement due to hunch-up.

Overall, ECC satisfies the requirements of pavement material from the compressive and flexural strength viewpoints. More importantly, high tensile strain capacity and bending deflection capacity make ECC feasible for jointless pavement.

Cracking Potential of ECC Under Restrained Shrinkage

For ECC material, drying shrinkage is greater than that of normal concrete, because of the absence of coarse aggregate (*12, 22*). Considering a slab with restraints at two ends, Li and Stang defined the restrained shrinkage cracking potential parameter, *P*, as expressed by Equation 2 (*23*):

$$P = \varepsilon_{sh} - (\varepsilon_e + \varepsilon_i + \varepsilon_{cp}) \quad (2)$$

where

ε_{sh} = free shrinkage strain of material,
ε_e = elastic tensile strain capacity,
ε_i = inelastic tensile strain capacity, and
ε_{cp} = tensile creep strain.

In Equation 2, ε_{sh} represents a deformation demand on the material, while $(\varepsilon_e + \varepsilon_i + \varepsilon_{cp})$ is the total material strain capacity.

If strain demand surpasses strain capacity, fracture failure initiates in the concrete material. Table 2 lists the typical range of cracking potential of normal concrete and ECC used in this study. The value of *P* for concrete was around 0, and it would be very possible to exceed 0 and lead to fracture. ECC exhibited a highly negative value of *P*, implying a large margin for suppressing fracture failure due to restrained drying shrinkage. In previous research, the cracking pattern of ECC under ring-restrained conditions verified the low crack potential for ECC material (*12, 24*). The extremely low cracking potential of ECC removes the size limitation for pavement slab due to drying shrinkage, thus achieving jointless function on highways.

Influence of Self-Healing on Recovery of Tensile Properties

Figure 5 shows the tensile stress–strain curve of an ECC specimen preloaded to 2% strain level and the reloading curve of a preloaded ECC specimen without self-healing. In the figure, the reloading stiffness without self-healing decreases significantly, compared with that of the preloaded specimen. The stiffness of ECC is defined as the slope in the initial elastic stage from the tensile strain–stress curve. Apart from stiffness, the tensile strain capacity also shows a great reduction when compared with that from the monotonic test.

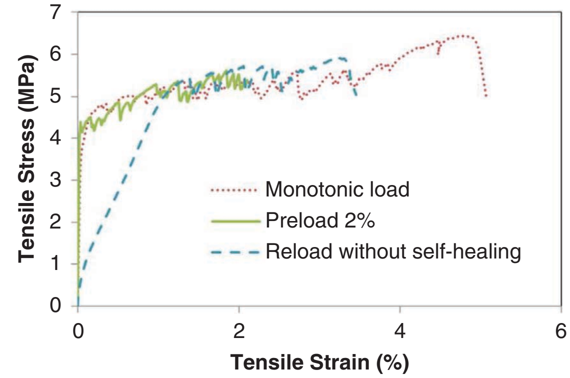

FIGURE 5 Relationship between tensile stress and strain of preload and reload specimens.

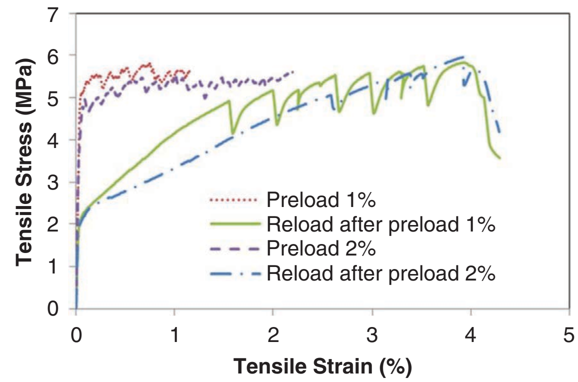

FIGURE 6 Tensile stress–strain curves of preload specimens after self-healing.

Figure 6 displays representative reloading tensile curves of ECC specimens after the self-healing process. After self-healing, the stiffness and tensile strain capacity of predamaged ECCs reveal obvious recovery compared with those without the self-healing process. The predamaged ECC specimens still have high tensile strain capacity of 4%, which is close to the control case (as shown in the table summarizing the mechanical properties of ECC).

The tensile performances of predamaged ECC specimens and the recovery level after the self-healing process are summarized in Table 3. As shown in the table, tensile behavior recovers better for the specimens with a lower level of predamage. For the two predamage levels, in tensile strain capacity, the ECCs recover 93% and 89% of the control case, respectively. The tensile strength of the predamaged specimen after self-healing reaches 5.8 and 5.9 MPa, respectively, which is at the same level as the control case. The

TABLE 2 Typical Strains and Cracking Potential of Normal Concrete and ECC

	ε_{sh} (%)	ε_e (%)	ε_i (%)	ε_{cp} (%)	*P*
Concrete	0.04–0.1	0.01	0	0.02–0.06	(–0.03) to 0.07
ECC	0.1–0.15	0.015	4.4	0.07	(–4.385) to (–4.335)

TABLE 3 Tensile Behavior of Predamaged ECC After Self-Healing

	Stiffness	Tensile Strain	Tensile Strength
To 1% of Tensile Strength (predamaged level)			
After reload	14.4 GPa	4.0%	5.8 MPa
Recovery level	92%	93%	100%
To 2% of Tensile Strength (predamaged level)			
After reload	15.7 GPa	3.9%	5.9 MPa
Recovery level	87%	89%	100%

stiffness of ECC recovers 92% and 87% of the control case, respectively. The recovery of mechanical performance of ECC after self-healing could maintain the integrity of pavement and the continuity of load transfer even after the appearance of cracks on the pavement.

Figure 7 plots the normalized RF value of the ECC specimens with wet-dry exposure cycles. Because of the crack damage for preloaded specimens, the normalized RF value of ECC has a large decline; it decreases to about 50% of that of the control specimen. For the two preloaded strain levels of ECC, the normalized RF values are very close in the self-healing process. Most of the RF increment happens before the three wet–dry cycles, after which additional RF recovery levels off. This phenomenon implies the self-healing process tends to happen fast for ECC pavement after crack damage. After 15 wet–dry exposure cycles, the RF values of all the preloaded specimens recover to 88% of that of the control specimens, demonstrating that the self-healing of ECC helps damaged ECC structures to recover. Thus, the self-healing behavior of ECC contributes toward reduced maintenance cost and extended pavement service life.

Influence of Self-Healing Behavior on Water Permeability

Figure 8 exhibits the evolution of the permeability coefficient (k) of the precracked ECC specimen with self-healing age. The figure shows that the water permeability coefficient of the precracked ECC specimen decreases gradually, from 6.8×10^{-8} m/s to 1.0×10^{-10} m/s over time, reflecting the self-healing products inside the cracked block water passage. After 15 days, the permeability coefficient of the cracked ECC specimens gradually stabilizes, implying that the crack space may be largely filled with self-healing products.

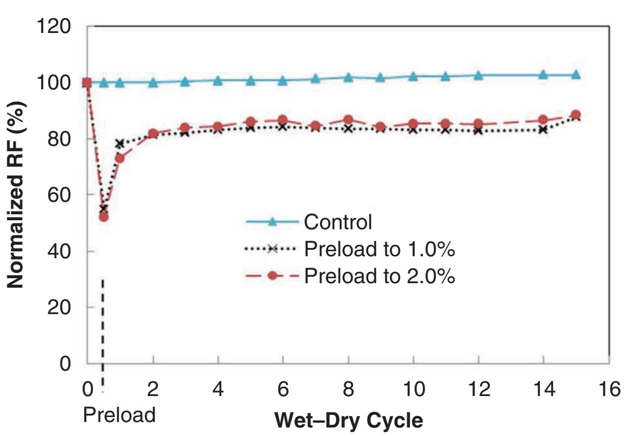

FIGURE 7 RF recovery of ECC under wet–dry cycles for different preload strain levels.

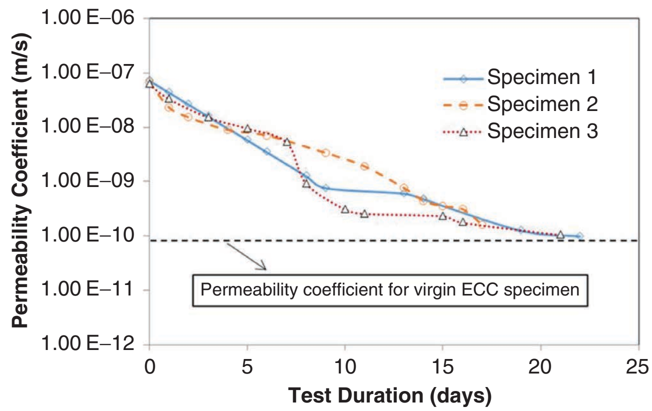

FIGURE 8 Evolution of the permeability coefficient of precracked ECC with self-healing age.

For comparison purposes, the permeability coefficient of virgin ECC was also measured. It was found that the permeability coefficient of virgin ECC is about 0.9×10^{-10} m/s, which is very close to that of cracked ECC with self-healing of 20 days. This result demonstrates that the self-healed ECC has the same capacity to prevent water pass-through as the virgin ECC does.

These results suggest that, because of self-healing behavior, ECC pavement is expected to prevent water from entering the subgrade or soil base even after cracking occurs, avoiding damage to the subgrade caused by water scour.

CONCLUSIONS

This paper proposes ECC with self-healing capacity as a candidate material for jointless concrete pavement. The study investigated the mechanical performance of ECC, cracking potential under restrained drying shrinkage, and ECC's self-healing behavior. The study revealed the feasibility of achieving jointless function for concrete pavement without the need for continuous steel reinforcement or prestressing. The following specific conclusions are drawn:

1. ECC exhibits high tensile strain capacity or deformability under tension or bending, instead of brittle failure mode for normal concrete. The flexural strength and compressive strength of ECC satisfy the requirements of concrete pavement, which are 12.2 and 45.8 MPa, respectively.
2. Because of its high tensile strain capacity, ECC shows highly negative values of P, which indicates a very low potential for fracture failure under restrained drying shrinkage.
3. With the help of self-healing products in predamaged ECC, its tensile performance (stiffness or tensile strain capacity or tensile strength), RF, and water permeability have a large recovery, approaching the same level as the control case (undamaged ECC).

ACKNOWLEDGMENTS

The authors graciously thank the Fundamental Research Funds for the Central Universities, the National Natural Science Foundation of China, for financial support for this work. The authors also thank the Chinese Scholarship Council for supporting the first author as a visiting scholar at the University of Michigan. The second author acknowledges the support of a start-up grant from Nanyang Technological University, Singapore.

REFERENCES

1. Li, V. C. From Micromechanics to Structural Engineering: The Design of Cementitious Composites for Civil Engineering Applications. *Japan Society of Civil Engineers Journal of Structural Engineering and Earthquake Engineering,* Vol. 10, No. 2, 1993, pp. 37–48.
2. Li, V. C. Engineered Cementitious Composites: Tailored Composites Through Micromechanical Modeling. In *Fiber Reinforced Concrete: Present and the Future* (N. Banthia, A. A. Bentur, and A. Mufti, eds.). Canadian Society for Civil Engineering, Montreal, Quebec, 1998, pp. 64–97.
3. Yu, J. T., J. H. Lin, Z. G. Zhang, and V. C. Li. Mechanical Performance of ECC with High-Volume Fly Ash After Sub-Elevated Temperatures. *Construction & Building Materials,* Vol. 99, 2015, pp. 82–89. https://doi.org/10.1016/j.conbuildmat.2015.09.002.
4. Li, V. C., C. Wu, S. Wang, A. Ogawa, and T. Saito. Interface Tailoring for Strain-Hardening Polyvinyl Alcohol-Engineered Cementitious Composite (PVA-ECC). *ACI Materials Journal,* Vol. 99, No. 5, 2002, pp. 463–472.
5. Zhang, Z. G., S. Z. Qian, and H. Ma. Investigating Mechanical Properties and Self-Healing Behavior of Micro-Cracked ECC with Different Volume of Fly Ash. *Construction & Building Materials,* Vol. 52, 2014, pp. 17–23. https://doi.org/10.1016/j.conbuildmat.2013.11.001.
6. Lepech, M. D., and V. C. Li. Water Permeability of Engineered Cementitious Composites. *Cement and Concrete Composites,* Vol. 31, No. 10, 2009, pp. 744–753. https://doi.org/10.1016/j.cemconcomp.2009.07.002.
7. Sahmaran, M., M. Li, and V. C. Li. Transport Properties of Engineered Cementitious Composites Under Chloride Exposure. *ACI Materials Journal,* Vol. 104, No. 6, 2007, pp. 604–611.
8. Wang, K., D. C. Jansen, P. S. Shah, and A. F. Karr. Permeability Study of Cracked Concrete. *Cement and Concrete Research,* Vol. 27, No. 3, 1997, pp. 381–393. https://doi.org/10.1016/S0008-8846(97)00031-8.
9. Yang, Y., M. D. Lepech, E.-H. Yang, and V. C. Li. Autogenous Healing of Engineered Cementitious Composites Under Wet-Dry Cycles. *Cement and Concrete Research,* Vol. 39, No. 5, 2009, pp. 382–390. https://doi.org/10.1016/j.cemconres.2009.01.013.
10. Keoleian, G. A., A. Kendall, J. E. Dettling, V. M. Smith, R. F. Chandler, M. D. Lepech, and V. C. Li. Life Cycle Modeling of Concrete Bridge Design: Comparison of Engineered Cementitious Composite Link Slabs and Conventional Steel Expansion Joints. *Journal of Infrastructure Systems,* Vol. 11, No. 1, 2005, pp. 51–60. https://doi.org/10.1061/(ASCE)1076-0342(2005)11:1(51).
11. Ma, H., S. Z. Qian, and Z. G. Zhang. Effect of Self-Healing on Water Permeability and Mechanical Property of Medium-Early-Strength Engineered Cementitious Composites. *Construction & Building Materials,* Vol. 68, 2014, pp. 92–101. https://doi.org/10.1016/j.conbuildmat.2014.05.065.
12. Zhang, Z. G., H. Ma, and S. Z. Qian. Investigation on Properties of ECC Incorporating Crumb Rubber of Different Sizes. *Journal of Advanced Concrete Technology,* Vol. 13, No. 5, 2015, pp. 241–251. https://doi.org/10.3151/jact.13.241.
13. Zhang, Z. G., Q. Zhang, S. Z. Qian, and V. C. Li. Low E-Modulus Early Strength Engineered Cementitious Composites Material: Development for Ultrathin Whitetopping Overlay. *Transportation Research Record: Journal of the Transportation Research Board,* No. 2481, 2016, pp. 41–47. https://dx.doi.org/10.3141/2481-06.
14. ASTM C109. *Standard Test Method for Compressive Strength of Hydraulic Cement Mortars.*
15. JSCE. *Recommendations for Design and Construction of High Performance Fiber Reinforced Cement Composites with Multiple Fine Cracks.* Japan Society of Civil Engineers, Tokyo, 2008.
16. ASTM C215. *Standard Test Method for Fundamental Transverse, Longitudinal, and Torsional Resonant Frequency of Concrete Specimens.*
17. Edvardsen, C. Water Permeability and Autogenous Healing of Cracks in Concrete. *ACI Materials Journal,* Vol. 96, No. 6, 1999, pp. 448–455.
18. Liu, H. Z., Q. Zhang, C. S. Gu, H. Z. Su, and V. C. Li. Influence of Micro-Cracking on the Permeability of Engineered Cementitious Composites. *Cement and Concrete Composites,* Vol. 72, 2016, pp. 104–113. https://doi.org/10.1016/j.cemconcomp.2016.05.016.
19. *Chinese Standard of Concrete Pavement Maintenance Technology.* JTJ-037, 2001.
20. *Chinese Standard of Highway Concrete Pavement Design.* JTG-D40, 2010.
21. Qian, S. Z., V. C. Li, H. Zhang, and G. A. Keoleian. Life Cycle Analysis of Pavement Overlays Made with Engineered Cementitious Composites. *Cement and Concrete Composites,* Vol. 35, No. 1, 2013, pp. 78–88. https://doi.org/10.1016/j.cemconcomp.2012.08.012.
22. Yang, E. H., Y. Z. Yang, and V. C. Li. Use of High Volumes of Fly Ash to Improve ECC Mechanical Properties and Material Greenness. *ACI Materials Journal,* Vol. 104, No. 6, 2007, pp. 620–628.
23. Li, V. C., and H. Stang. Elevating FRC Material Ductility to Infrastructure Durability. *Proceedings of RILEM International Symposia on Fiber Reinforced Concrete,* 2004, pp. 171–86.
24. Huang, X., R. Ranade, W. Ni, and V. C. Li. On the Use of Recycled Tire Rubber to Develop Low E-Modulus ECC for Durable Concrete Repairs. *Construction & Building Materials,* Vol. 46, 2013, pp. 134–141. https://doi.org/10.1016/j.conbuildmat.2013.04.027.

The Standing Committee on Design and Rehabilitation of Concrete Pavements peer-reviewed this paper.